CrossMark

Revisiting the Evidence for an Intermediate-mass Black Hole in the Center of NGC 6624 with Simulations

Li-Chun Wang[1,2] and Yi Xie[1]
[1] School of Science, Jimei University, Xiamen 361021, China; xieyi@jmu.edu.cn
[2] Physics Experiment Center, Jimei University, Xiamen 361021, China

Abstract

The acceleration of LMXB 4U 1820-30 derived from its orbital-period derivative $\dot{P}_b$ was supposed to be the evidence for an Intermediate-mass black hole (IMBH) in the Galactic globular cluster (GC) NGC 6624. However, we find that the anomalous $\dot{P}_b$ is mainly due to the gravitational wave emission, rather than the acceleration in cluster potential. Using the standard structure models of GCs, we simulate acceleration distributions for pulsars in the central region of the cluster. By fitting the acceleration of J1823-3021A with the simulated distribution profiles (maximum values), it is suggested that an IMBH with mass $M \gtrsim 950^{+550}_{-350} M_{\odot}$ may reside in the cluster center. We further show that the second period derivative $\ddot{P}$ of J1823-3021A is probably due to the gravitational perturbation of a nearby star.

1. Introduction

Globular clusters (GCs) are composed of $\sim 10^3$–10^5 old stars in regions from tens to hundreds of light years across. They are self-gravitating spherical systems, and become more dense and brighter toward the center. Many studies indicated that Intermediate-mass black holes (IMBHs) $(M \sim 10^2$–$10^5 M_{\odot})$, which are important evolution links between stellar-mass black holes (BHs) and super-massive black holes (SMBHs), should form and reside in dense stellar systems, mainly in the cores of GCs, and also in some dwarf galaxies (Sigurdsson & Hernquist 1993; Ebisuzaki et al. 2001; Miller & Hamilton 2002; Barth et al. 2004, 2005; Greene & Ho 2006; Haiman et al. 2013). Therefore, some dedicated observations have been performed to search IMBHs in the central regions of the GCs. If confirmed, the evidence would have manifold effects on several basic astrophysical problems, such as GC dynamics, the origin of ultraluminous X-ray sources and gravitational wave events (Fragione et al. 2018).

There are two schemes that widely used to reveal the presence of IMBHs in GCs: studying the dynamics of stars and looking for signatures of accretion. However, the existence of IMBHs is still uncertain, and some controversial results were obtained (Maccarone 2004; Pooley & Rappaport 2006; McLaughlin et al. 2006; de Rijcke et al. 2006; Noyola et al. 2008; van der Marel & Anderson 2010; Miller-Jones et al. 2012; Lützgendorf et al. 2013; Sun et al. 2013; Baumgardt 2017; Kızıltan et al. 2017; Tremou et al. 2018; Baumgardt et al. 2019; Aros et al. 2020). Recently, a luminous X-ray burst from a tidal disruption event in

an extragalactic star cluster provides that it may contain an IMBH with $M \sim 10^4 M_{\odot}$ (Lin et al. 2018).

The bulge GC NGC 6624 is one of the most massive and dense clusters located $\sim$1.2 kpc away from the Galactic Center and $\sim$7.9 kpc away from the Earth (Harris 1996). Due to the cusp signature of optical observations for the radial density profile, it is considered to be a core-collapsed cluster (Sosin & King 1995). To date, 11 pulsars have been discovered in the cluster (Biggs et al. 1994; Knight et al. 2005; Knight 2007; Freire et al. 2011; Lynch et al. 2012; Perera et al. 2017a; Abbate et al. 2020, 2022; Ridolfi et al. 2021), and another pulsar J1823-3022 is not yet confirmed as an association with the GC due to its long period and large offset from the cluster center (Abbate et al. 2022). All of the confirmed pulsars in the cluster have period measurements, and only four of them have period time derivative measurements: PSRs J1823-3021A, B, C, and G. It also contains the low-mass X-ray binary (LMXB) 4U 1820-30, which is the brightest object in X-ray band in the cluster, with extremely short orbital period and an anomalously larger orbital period derivative (van der Klis et al. 1993; Chou & Grindlay 2001; Peuten et al. 2014).

Analyzing long-term timing of 4U 1820–30 with unprecedented accuracy, Peuten et al. (2014) measured the orbital period and its first derivative, $P = (685.01197 \pm 0.00003)$s and $\dot{P} = (-1.15 \pm 0.06) \times 10^{-12}$ s s^{-1}, which yields $\dot{P}/P = (-5.3 \pm 0.3) \times 10^{-8}$ yr^{-1}. The significant negative $\dot{P}$ was explained as there is a very large amount of dark remnants contained in the center of NGC 6624. Perera et al. (2017a, 2017b) further suggested that the cluster may contain

an IMBH with the minimum model-dependent mass $\sim 2 \times 10^4 M_{\odot}$, based on the timing data of 4U 1820-30 and PSR B1820-30A. However, the observed period changes of PSR B1820-30A can also be explicated with a cluster model without an IMBH (Gieles et al. 2018), the dynamical model has a very high core density $\rho_c = 7.54^{+34.3}_{-5.56} \times 10^7 M_{\odot} \mathrm{pc}^{-3}$. Comparing N-body simulations with the cluster, Baumgardt et al. (2019) claimed that the model with an IMBH of $M \gtrsim 1000 M_{\odot}$ are incompatible with the optical observation constraints. Although evidence has been accumulating, there is still no uncontroversial case for the existence of IMBHs in any Galactic GCs.

In this work, we simulate the absolute values of the mean-field acceleration for pulsars in NGC 6624, with published density profile and core radius of the cluster (Harris 1996). We fit the measured accelerations of J1823-3021A with the simulated maximum values. This method can provide a minimum mass of the IMBH in the center of the cluster more precisely. In Section 2 we describe the methods of the simulations, and the results are given in Section 3. Our conclusions and discussions are presented in Section 4.

2. Methods

We first build a coordinate system for the convenient description, as shown in Figure 1. The plane perpendicular to our line-of-sight and passing through the center of gravity (CoG) of the cluster is defined as O. The projected distance of a pulsar from the CoG in plane O as $R'_{\perp}$. The line-of-sight distance between the pulsar and plane O as l, and r' is the radial distance of the pulsar from the GC center, $r' = \sqrt{R'^2_{\perp} + l^2}$.

An IMBH strongly affects the spatial distribution of stars around it in the central region. The central IMBH with mass M_{BH} have a radius of influence (Baumgardt et al. 2004a),

$$r_i = \frac{3 M_{\mathrm{BH}}}{8 \pi \rho_c r_c^2}, \quad (1)$$

where r_c is the core radius of the GC, and ρ_c is the core density. At r_i and beyond, the density profile are strongly setted by the standard King model (King 1962),

$$\rho(r') \simeq \rho_c [1 + (r'/r_c)^2]^{-\frac{3}{2}}. \quad (2)$$

Within r_i, the star distribution is influenced dominantly by the IMBH, the density profile obeys $\rho_{\mathrm{BH}} \propto r^{-\alpha}$ (Prager et al. 2017), which is particularly suited for cusp clusters (Djorgovski & King 1986). Numerical simulations of clusters with an IMBH in the center found that the power index $\alpha = 1.55$ (Baumgardt et al. 2004b). The total interior mass of stars with contribution at any given radius r'_* can be obtained by radially integrating the density profiles. Multiplying G/r'^2_* yields the
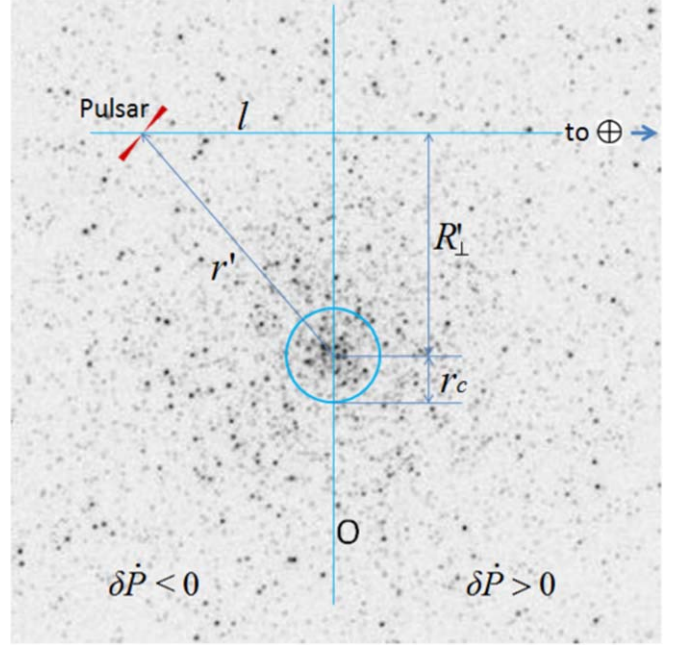

Figure 1. Schematic illustration of the location of a pulsar with respect to the center of the cluster NGC 6624. The optical image of the cluster is taken from the Hubble Space Telescope (https://hla.stsci.edu/). The plane of the sky passing through the CoG of the cluster is defined as O, l is the line-of-sight distance between the pulsar and plane O, $R'_{\perp}$ is the projected separation between a pulsar and CoG on the plane of the sky, r' is the radial distance of the pulsar from the GC center, and r_c is the core radius of the cluster. When a pulsar lies in the back half of the cluster, the GC potential contributes a negative value on the period of the pulsar, i.e., $\delta \dot{P} < 0$.

acceleration felt at r'_*, which reads (Xie & Wang 2020)

$$a(r'_*) = \frac{4\pi G}{r'^2_*} [M_{\mathrm{BH}}/4\pi + \int_0^{r_i} r'^2 \rho_{\mathrm{BH}} dr' + \int_{r_i}^{r'_*} r'^2 \rho(r') dr']. \quad (3)$$

The mean-field line-of-sight acceleration a_l can be obtained via projecting the acceleration $a(r'_*)$ along the line-of-sight direction, i.e., $a(r'_*)$ is multiplied by a factor of l/r'_*. It is apparent that only the stars interior to r'_* are accounted for the acceleration of each pulsar, given the probabilities that the nearest stars contribute to different pulsars (occurring flyby events) at the same time are negligible (Peuten et al. 2014; Prager et al. 2017).

In order to obtain a_l for pulsars at various $R'_{\perp}$ of the central region, Monte Carlo simulations are performed for a complete profile of a_l distribution. Due to the effect of mass segregation (Spitzer 1987), some heavier stellar population like pulsars are centrally concentrated, thus their timing is in favor of giving us insights into the innermost regions of the cluster. It is well confirmed by the locations of reported pulsars, such as these in GCs Terzan 5 and 47 Tucanae. In the circumstances, the observed column number density of the depositing pulsars is

given by Lugger et al. ([1995]):

$$n(x_\perp) = n_0(1 + x_\perp^2)^{\beta/2}. \tag{4}$$

in which n_0 is the central number density. $x_\perp \equiv R'_\perp/r_c$, is the distance away from the CoG in O plane in unit of the core radius of the cluster. β is the parameter on the mass segregation, which is preseted to obey a Gaussian distribution, with center value of -3 and dispersion of 0.5 (Abbate et al. [2019]; Wang & Xie [2021]).

Due to the Doppler effect, the spin period derivatives of pulsars are linked to the line-of-sight accelerations by the equation (Phinney [1993]; Prager et al. [2017])

$$\frac{\dot{P}}{P} = \frac{\dot{P}_0}{P_0} + \frac{a_l}{c} + \frac{a_g}{c} + \frac{a_s}{c} + \frac{a_{DM}}{c}, \tag{5}$$

in which $\dot{P}_0/P_0$ is the intrinsic spin-down due to the pulsar's magnetic braking, a_g is the acceleration from the Galactic potential on a pulsar, a_s is the centrifugal acceleration caused by the Shklovskii effect, a_{DM} is the apparent acceleration due to the variations of dispersion measure (DM), c is the speed of light. For NGC 6624, the calculated value of the galactic acceleration is $a_g/c = -5.7 \times 10^{-11}$ yr^{-1} (Peuten et al. [2014]). The Shklovskii effect for a pulsar in the cluster is $a_s/c = \mu^2 D/c \approx 5.89 \times 10^{-11}$ yr^{-1} (Perera et al. [2017a]), where μ is the proper motion of the pulsar, D kpc is the pulsar distance (Kuulkers & den Hartog [2003]). The apparent acceleration from the stochastic DM error is (Prager et al. [2017])

$$a_{DM} = -6.1 \times 10^{-14} \left(\frac{\Delta t_{DM}}{1\,\mu s}\right)\left(\frac{10\,yr}{T}\right)^2, \tag{6}$$

in which Δt_{DM} is the dispersive delay time, T is the timescale for the DM measurement. For a delay of $\Delta t_{DM} = 100\,\mu s$ and $T = 10$ yr, the apparent acceleration is $a_{DM}/c = -6.4 \times 10^{-15}$ yr^{-1}. The line-of-sight acceleration a_l depends on the cluster mass within the given radius. At the position of 4U 1820-30, the cluster acceleration is estimated to be $a_l/c = 1.3 \times 10^{-9}$ yr^{-1} (Prodan & Murray [2012]). Therefore, a_g, a_s, and a_{DM} are all much smaller than a_l, and have very minor contributions to the measured acceleration. Then, Equation ([5]) can be reduced to

$$\frac{\dot{P}}{P} \approx \frac{\dot{P}_0}{P_0} + \frac{a_l}{c}. \tag{7}$$

To evaluate the intrinsic spin-down term, we use the median values of the pulsar's P_0 and $\dot{P}_0$ taken from the Australian Telescope National Facility (ATNF) catalog[3] (Manchester et al.[2005]). For millisecond pulsars, the moderate value of $\dot{P}_0/P_0 \sim 10^{-10}$ yr^{-1}. For normal radio pulsar, the value is $\sim 5 \times 10^{-8}$ yr^{-1}. While the magnitude of a_l/c could be $\sim 10^{-8}$ yr^{-1} near the center of the cluster (Chou & Grindlay [2001]; Gieles et al. [2018]). Thus, $\dot{P}_0/P_0$ can be neglected only for millisecond pulsars, i.e., $\dot{P}/P \simeq a_l/c$.

This relation can be used to test the gravitational potential for the central regions of GCs.

Similar to Equation ([7]), we can express the orbital-period derivative for LMXBs or pulsar binaries as follows:

$$\frac{\dot{P}_b}{P_b} = \left(\frac{\dot{P}_b}{P_b}\right)_{GR} + \frac{a_l}{c}, \tag{8}$$

where $(\dot{P}_b/P_b)_{GR}$ is the orbital decay due to gravitational wave emission. For wide binary systems, the GR term is negligible, the orbital period P_b and orbital period derivatives $\dot{P}_b$ are very suitable to probe the cluster potential, since $\dot{P}_b$ is almost completely caused by the cluster potential. Thus Equation ([8]) may reduce to $\dot{P}_b/P_b \simeq a_l/c$. However, the GR term may be significant for tight binaries, and it has been taken into account in many studies (Matthews et al. [2016]; Perera et al. [2019]). The X-ray source 4U 1820-30 is in a compact binary system (with a period of ~ 685 s), consisting of a white dwarf of $6.89 \times 10^{-2}\,M_\odot$ accreting onto a neutron star of $1.58\,M_\odot$ (Güver et al. [2010]; Suvorov [2021]), with an orbit of eccentricity $\lesssim 0.004$ (Zdziarski et al. [2007]). Using Equation (8.52) in Lorimer & Kramer [2012], we obtained that the expected $(\dot{P}_b)_{GR}$ is about -6.3×10^{-12} yr^{-1}, and $(\dot{P}_b/P_b)_{GR} \simeq -2.9 \times 10^{-7}$ yr^{-1}. It is apparent that the General Relativity effect is the dominant term. Its absolute value is apparently greater than the value of the observed $\dot{P}_b/P_b \simeq -5.3 \times 10^{-8}$ yr^{-1}. Part of the reasons may be the accretion process. The secondary (helium dwarf) transfers matter to the accretion disk of the neutron star, which would cause a positive period derivative (Rappaport et al. [1987]). Nevertheless, 4U 1820-30 is currently unsuitable for testing the GC potential.

3. Results

There are four pulsars, J1823-3021A, B, C, and G with measured P and $\dot{P}$, and the LMXB 4U 1820-30 with measured P_b and $\dot{P}_b$ in NGC 6624,[4] as shown in Table [1]. J1823-3021B and J1823-3021C are normal pulsars, $\dot{P}_0/P_0$ of J1823-3021G is too small (implies the pulsar is located very far away from or very close to the plane O, i.e., a very large or small l), $\dot{P}_b$ of 4U 1820-30 is contributed dominantly by gravitational wave emission and accretion process, thus only J1823-3021A is suitable for testing the gravitational field of the cluster.

To obtain the accelerations of pulsars at different locations in NGC 6624, we take the precise values of the central density and the core radius determined from optical observations as $\rho_c = 1.12 \times 10^5\,M_\odot pc^{-3}$ and $r_c = 0.14$ pc, respectively (Harris [1996]). We calculate the line-of-sight accelerations (a_l) caused by the gravitational potential of NGC 6624 with Equations ([1])–([4]). We perform Monte Carlo simulations on the line-of-sight accelerations caused by the gravitational

---

Table 1
List of Pulsars with Reported Period and Its First Derivative in NGC 6624

Pulsar	P	$\dot{P}$	$\dot{P}/P$ $(10^{-8}$	$R'_\perp$	Reference
	(ms)	$(10^{-19}$ s s$^{-1})$	yr$^{-1})$	(pc)	
J1823-3021A	5.44	33.85(1)	1.96	0.018(4)	1,2
J1823-3021B	378.6	315(3)	0.26	0.516	1,3
J1823-3021C	405.9	2240(25)	1.74	0.340	3
J1823-3021G	6.09	−0.18(2)	0.04	0.188	4
4U 1820-30	*	*	*	0.050	5

Note.
[a] The orbital period and its time derivative of LMXB 4U 1820–30 are $P_b = 685.01$s and $\dot{P}_b = -1.15 \pm 0.06 \times 10^{-12}s\,s^{-1}$, which is translated into $\dot{P}_b/P_b = (-5.3 \pm 0.3) \times 10^{-8}$ yr^{-1} (Peuten et al. 2014).

References: (1) Biggs et al. (1994); (2) Freire et al. (2011); (3) Lynch et al. (2012); (4) Ridolfi et al. (2021); (5) Peuten et al. (2014).

potential of NGC 6624, for pulsars in the innermost region of the GC. The simulated a_l distribution is displayed in Figure 2. One can see that the maximum line-of-sight accelerations, $|a_l/c| \lesssim 0.05 \times 10^{-8}$ yr^{-1}. The simulated results are about two orders of magnitude lower than the reported results of J1823-3021A ($\sim 2 \times 10^{-8}$ yr^{-1}). Therefore, the mass distribution inferred from the cluster surface brightness cannot explain the acceleration derived from $\dot{P}/P$ of J1823-3021A. To understand this, an IMBH is contained in the center or a large amount of dark remnants concentrated in the central area, may be the two most plausible scenarios.

For the models, we vary the mass of the central IMBH, while holding all the other cluster parameters constant. We then use the maximum values of the simulated results to fit the acceleration of J1823-3021A. As shown in Figure 3, the inferred minimum mass of the IMBH is $950^{+550}_{-350}\,M_\odot$. The uncertainty is obtained by fitting the error bar of the projected distance of the pulsar from the cluster center. It suggests that an invisible mass of $\sim 950\,M_\odot$ is embedded in a radius of ~ 0.02 pc, providing a mass density of $\gtrsim 1.3 \times 10^8\,M_\odot\mathrm{pc}^{-3}$. The high-eccentricity orbit of the pulsar reveals the total enclosed mass $M_t \gtrsim 7.5 \times 10^3\,M_\odot$ (Perera et al. 2017a), and the averaged mass density $\gtrsim 10^9\,M_\odot\mathrm{pc}^{-3}$. Such a high averaged mass density can be interpreted naturally if there is an IMBH in the center, and seems unlikely for the dark remnant scenario.

It is also possible that the unusual $\dot{P}$ value for J1823-3021A is due to flyby objects in the cluster with its high stellar density, as suggested by Gieles et al. (2018). The pulsar will experience a time-varying acceleration due to the passing star, which may produce an anomalous $\ddot{P}$, as $\ddot{P}/P = \dot{a}/c$ (Blandford et al. 1987). The pulsar acceleration contributed by the close encounter with the nearest star $\sim GM_t/b^2$. The average

interstellar distance within the radius is $b \sim (3M_s/4\pi\rho_c)^{1/3}$, where M_s is the mass of the star. The acceleration can be estimated as

$$\frac{a}{c} \sim \frac{GM_t}{(3M_s/4\pi\rho_c)^{2/3}} \simeq 8.2 \times 10^{-9}\ \mathrm{yr}^{-1}$$
$$\times \left(\frac{M_t}{100\,M_\odot}\right)\left(\frac{M_s}{1\,M_\odot}\right)^{-2/3}\left(\frac{\rho_c}{10^5\,M_\odot\mathrm{pc}^{-3}}\right)^{2/3}. \quad (9)$$

One can get $a/c \sim 8.2 \times 10^{-9}$ yr^{-1} for the typical values of the parameters, which is about one third of the observed $\dot{P}/P$. The timescale of the encounter can be estimated as $\tau \sim b/\sigma$, where σ is the velocity dispersion of stars in the region. Accordingly, $\ddot{P}/P \sim a/\tau c$ can be expressed as

$$\frac{\ddot{P}}{P} \sim \frac{4\pi G\sigma}{3c}\frac{M_t}{M_s}\rho_c \simeq 1.4 \times 10^{-26}\ \mathrm{s}^{-2}$$
$$\times \left(\frac{\sigma}{10\ \mathrm{km\ s}^{-1}}\right)\left(\frac{M_t}{100\,M_\odot}\right)\left(\frac{M_s}{1\,M_\odot}\right)^{-1}\left(\frac{\rho_c}{10^5\,M_\odot\mathrm{pc}^{-3}}\right). \quad (10)$$

One can get $\ddot{P} = 7.6 \times 10^{-29}$ s^{-1} for the typical values of the parameters. It is sufficient to explain the observed value of the second derivative of the spin period, $\ddot{P}_{obs} = -1.7 \times 10^{-29}$ s^{-1} (Freire et al. 2011). Since the predicted $\dot{P}/P$ is much smaller, while the predicted $\ddot{P}/P$ is greater than four times of the observed values for the same parameters, we conclude that the observed $\dot{P}/P$ is mainly due to the central IMBH, however, the observed $\ddot{P}/P$ is probably due to the gravitational perturbation of a flyby object, i.e., it is possible that the pulsar has a close encounter with a nearby star. Thus we confirm that $\dot{P}$ is dominated by smooth underlying potential, and $\ddot{P}$ can be used to infer stochastic effects. The best-fitting dynamical models of Gieles et al. (2018) obtained a very high central density, $\rho_c = 7.54^{+34.3}_{-5.56} \times 10^7\,M_\odot\mathrm{pc}^{-3}$. It corresponds to $\ddot{P} = 2.6 \times 10^{-26}$ s^{-1}, and can hardly match with the observed value.

4. Discussions and Conclusions

Theoretical models suggested that IMBHs may form in the central regions of GCs, however, they are still elusive to observations. The timing effects of pulsar accelerations may supply unique tests on the cluster gravitational fields. Based on standard structure models of the GCs, we simulated the acceleration distributions of pulsars in the central region of NGC 6624. By fitting the reported $\dot{P}/P$ of J1823-3021A, we find that an IMBH with $M \gtrsim 950^{+550}_{-350}\,M_\odot$ may be located at the cluster center. Compared with the previous approach that fitting the reported data to Equation (7) of Peuten et al. (2014), our method effectively avoids its mathematical approximation (up to $\sim 50\%$ (Phinney 1993)), as well as the measurement errors on the line-of-sight velocity dispersion $\sigma(R_\perp)$ of giant stars at the pulsar position.
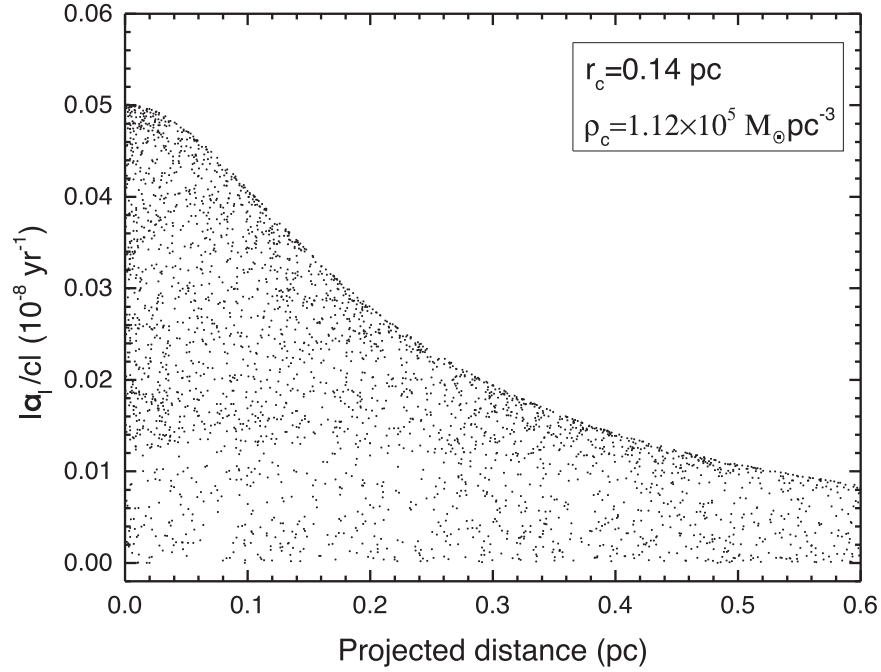
Figure 2. The simulated a_l due to the gravitational potential of NGC 6624, for pulsars in the innermost region of the GC. The core density $\rho_c = 1.12 \times 10^5\,M_\odot\mathrm{pc}^{-3}$ and the core radius $r_c = 0.14$ pc are taken and no IMBH is considered in the simulation.
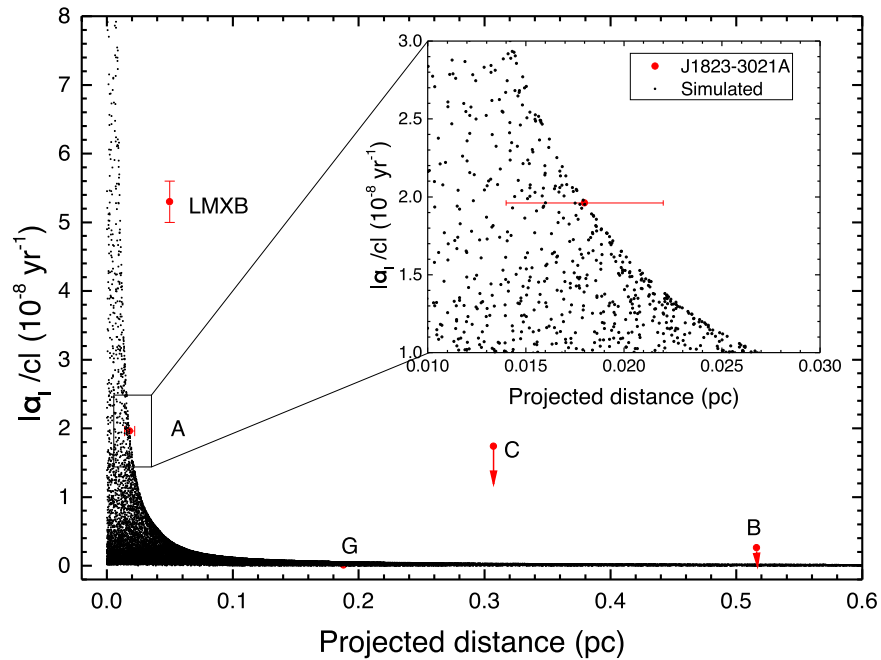

Figure 3. The line-of-sight acceleration a_l vs. the projected radius $R'_\perp$. The measured accelerations along the line of sight for pulsars J1823-3021A, J1823-3021B, J1823-3021C, J1823-3021G, and LMXB 4U 1820-30 are represented by red points and marked appropriately. The simulated line-of-sight accelerations, which caused by the gravitational potential of NGC 6624 with an additional IMBH of 950 $M_\odot$, are represented by black circles.

We found that the second period derivative of J1823-3021A is probably due to a close encounter with a nearby star of the cluster, as previously proposed in literature (Peuten et al. 2014; Gieles et al. 2018). $\dddot{P}_{\rm obs}$ agrees well with the expectation of the model with $\rho_c \sim 10^5\,M_\odot {\rm pc}^{-3}$. We thus confirmed that $\ddot{P}$ can be used to infer gravitational perturbations (Blandford et al. 1987). We showed that the orbital-period derivative of 4U 1820–30 is dominated by the effects of the gravitational wave emission and accretion process. Thus it is unsuitable to be used to probe the GC potential. J1823-3021C is also analyzed by Peuten et al. (2014) and Perera et al. (2017a), and an IMBH with mass of $6 \times 10^4\,M_\odot$ was derived. However, the acceleration derived from its $\dot{P}/P$ cannot be used directly to estimate the gravitational potential of the cluster (Perera et al. 2017b), since J1823-3021C is a normal pulsar, whose $\dot{P}_0/P_0$ term is usually dominating. To find further evidence for the central IMBH of this cluster, more long-term data may require with other analyzing methods/techniques.

Acknowledgments

References

Abbate, F., Bailes, M., Buchner, S. J., et al. 2020, MNRAS, 498, 875
Abbate, F., Possenti, A., Colpi, M., et al. 2019, ApJL, 884, L9
Abbate, F., Ridolfi, A., Barr, E. D., et al. 2022, MNRAS, 513, 2292
Aros, F. I., Sippel, A. C., Mastrobuono-Battisti, A., et al. 2020, MNRAS, 499, 4646
Barth, A. J., Greene, J. E., & Ho, L. C. 2005, ApJL, 619, L151
Barth, A. J., Ho, L. C., Rutledge, R. E., et al. 2004, ApJ, 607, 90
Baumgardt, H. 2017, MNRAS, 464, 2174
Baumgardt, H., He, C., Sweet, S. M., et al. 2019, MNRAS, 488, 5340
Baumgardt, H., Makino, J., & Ebisuzaki, T. 2004a, ApJ, 613, 1133
Baumgardt, H., Makino, J., & Ebisuzaki, T. 2004b, ApJ, 613, 1143
Biggs, J. D., Bailes, M., Lyne, A. G., et al. 1994, MNRAS, 267, 125
Blandford, R. D., Romani, R. W., & Applegate, J. H. 1987, MNRAS, 225, 51P
Chou, Y., & Grindlay, J. E. 2001, ApJ, 563, 934
de Rijcke, S., Buyle, P., & Dejonghe, H. 2006, MNRAS, 368, L43
Djorgovski, S., & King, I. R. 1986, ApJL, 305, L61
Ebisuzaki, T., Makino, J., Tsuru, T. G., et al. 2001, ApJL, 562, L19
Fragione, G., Ginsburg, I., & Kocsis, B. 2018, ApJ, 856, 92
Freire, P. C. C., Abdo, A. A., Ajello, M., et al. 2011, Sci, 334, 1107
Gieles, M., Balbinot, E., Yaaqib, R. I. S. M., et al. 2018, MNRAS, 473, 4832
Greene, J. E., & Ho, L. C. 2006, ApJL, 641, L21
Güver, T., Wroblewski, P., Camarota, L., et al. 2010, ApJ, 719, 1807
Haiman, Z., Tanaka, T., Fernandez, R., et al. 2013, SnowPAC 2013—Black Hole Fingerprints: Dynamics, Disruptions and Demographics, 2
Harris, W. E. 1996, AJ, 112, 1487
King, I. 1962, AJ, 67, 471
Kızıltan, B., Baumgardt, H., & Loeb, A. 2017, Natur, 542, 203
Knight, H. S. 2007, MNRAS, 378, 723
Knight, H. S., Bailes, M., Manchester, R. N., et al. 2005, ApJ, 625, 951
Kuulkers, E., den Hartog, P. R., in't Zand, J. J. M., et al. 2003, A&A, 399, 663
Lin, D., Strader, J., Carrasco, E. R., et al. 2018, NatAs, 2, 656
Lorimer, D. R., & Kramer, M. 2012, in Handbook of Pulsar Astronomy, ed. D. R. Lorimer & M. Kramer (Cambridge: Cambridge Univ. Press)
Lugger, P. M., Cohn, H. N., & Grindlay, J. E. 1995, ApJ, 439, 191
Lützgendorf, N., Kissler-Patig, M., Gebhardt, K., et al. 2013, A&A, 552, A49
Lynch, R. S., Freire, P. C. C., Ransom, S. M., et al. 2012, ApJ, 745, 109
Maccarone, T. J. 2004, MNRAS, 351, 1049
Manchester, R. N., Hobbs, G. B., Teoh, A., et al. 2005, AJ, 129, 1993
Matthews, A. M., Nice, D. J., Fonseca, E., et al. 2016, ApJ, 818, 92
McLaughlin, D. E., Anderson, J., Meylan, G., et al. 2006, ApJS, 166, 249
Miller, M. C., & Hamilton, D. P. 2002, MNRAS, 330, 232
Miller-Jones, J. C. A., Wrobel, J. M., Sivakoff, G. R., et al. 2012, ApJL, 755, L1
Noyola, E., Gebhardt, K., & Bergmann, M. 2008, ApJ, 676, 1008
Perera, B. B. P., Barr, E. D., Mickaliger, M. B., et al. 2019, MNRAS, 487, 1025
Perera, B. B. P., Stappers, B. W., Lyne, A. G., et al. 2017a, MNRAS, 468, 2114
Perera, B. B. P., Stappers, B. W., Lyne, A. G., et al. 2017b, MNRAS, 471, 1258
Peuten, M., Brockamp, M., Küpper, A. H. W., et al. 2014, ApJ, 795, 116
Phinney, E. S. 1993, Structure and Dynamics of Globular Clusters, 50, 141
Pooley, D., & Rappaport, S. 2006, ApJL, 644, L45
Prager, B. J., Ransom, S. M., Freire, P. C. C., et al. 2017, ApJ, 845, 148
Prodan, S., & Murray, N. 2012, ApJ, 747, 4
Rappaport, S., Nelson, L. A., Ma, C. P., et al. 1987, ApJ, 322, 842
Ridolfi, A., Gautam, T., Freire, P. C. C., et al. 2021, MNRAS, 504, 1407
Sigurdsson, S., & Hernquist, L. 1993, Natur, 364, 423
Sosin, C., & King, I. R. 1995, AJ, 109, 639
Spitzer, L. 1987, Dynamical Evolution of Globular Clusters (Princeton, NJ: Princeton Univ. Press), c1987
Sun, M.-Y., Jin, Y.-L., Gu, W.-M., et al. 2013, ApJ, 776, 118
Suvorov, A. G. 2021, MNRAS, 503, 5495
Tremou, E., Strader, J., Chomiuk, L., et al. 2018, ApJ, 862, 16
van der Klis, M., Hasinger, G., Verbunt, F., et al. 1993, A&A, 279, L21
van der Marel, R. P., & Anderson, J. 2010, ApJ, 710, 1063
Wang, L.-C., & Xie, Y. 2021, RAA, 21, 270
Xie, Y., & Wang, L.-C. 2020, RAA, 20, 191
Zdziarski, A. A., Wen, L., & Gierliński, M. 2007, MNRAS, 377, 1006